Experimental investigation of the statistical distribution of single atoms in cavity quantum electrodynamics

2015 Laser Phys. Lett. 12 065501

(http://iopscience.iop.org/1612-202X/12/6/065501)

IOP Publishing | Astro Ltd
Laser Physics Letters
Laser Phys. Lett. **12** (2015) 065501 (4pp)
doi:10.1088/1612-2011/12/6/065501

Experimental investigation of the statistical distribution of single atoms in cavity quantum electrodynamics

Jin-Jin Du, Wen-Fang Li, Rui-Juan Wen, Gang Li and Tian-Cai Zhang

State Key Laboratory of Quantum Optics and Quantum Optics Devices, Institute of Opto-Electronics, Shanxi University, Taiyuan 030006, People's Republic of China

E-mail: tczhang@sxu.edu.cn

Received 18 March 2015, revised 20 April 2015
Accepted for publication 22 April 2015
Published 11 May 2015

Abstract

The Hanbury Brown–Twiss experiment for a beam of photons or atoms can be performed using counting experiments. We present the statistical distribution of single ^{133}Cs atoms detected by a high finesse microcavity, which acts as a point-like single-atom counter. The distribution of the arrival times of the atoms and the correlation between the atoms was obtained based on the full counting statistics of the beam emitted from the cavity. The bunching behavior of the thermal atomic beams is clearly observable using this type of atom–cavity system. The correlation between the cesium atoms depends on the temperature of the atom cloud, and the corresponding parameters may be found by fitting an experimentally measured curve using the theory of multimode thermal light.

Keywords: laser cooling and trapping, atomic beam sources and detectors, cavity quantum electrodynamics

(Some figures may appear in colour only in the online journal)

1. Introduction

About half a century ago, Hanbury Brown and Twiss (HBT) were the first to discover intensity correlations between photons from the radiation of a gaseous discharge [1], and to use this phenomenon of photon bunching in light emitted by a chaotic source to measure the angular size of a star [2]. This milestone stimulated the birth of modern quantum optics [3]. Advances in atom cooling and detection have pushed forward the observation and full characterization of the atomic analogue of the HBT effect with bosonic atoms [4–8]. Early experiments measuring this effect in neutral atoms were realized by coupling an atom (laser) beam out of a Bose–Einstein condensate. Similarly, a time-resolved and position-sensitive detector (microchannel plate and delay-line anode) has been applied to detect single atoms to compare the HBT effect in bosons and fermions [9]. In 2005, a high-finesse optical enabled cavity was employed to detect the time-resolved counting of single atoms extracted from a weakly interacting Bose–Einstein condensate of ^{87}Rb atoms. This was based on the measurement of the second-order correlation function $g^2(\tau)$ of an atom laser and pseudo-thermal atomic beams in an HBT type experiment, where τ is the time delay [6]. Sensitive probing and manipulation of single atoms with the quantized electromagnetic field in the cavity mode is possible in the strong coupling regime of a cavity quantum electrodynamics (QED) system, where the decoherence is much smaller than the coupling [10–13]. In this letter we describe an experiment in which we also counted single atoms using a high finesse optical microcavity, but the atomic beam is directly derived from a magneto-optical trap (MOT). The second-order correlation function of this truly thermal atomic beam is obtained using the HBT effect, and its bunching behavior is observed.

2. Experimental setup and results

Our experimental setup is shown in figure 1. The main components of the MOT and microcavity were placed in a vacuum chamber where the pressure in the

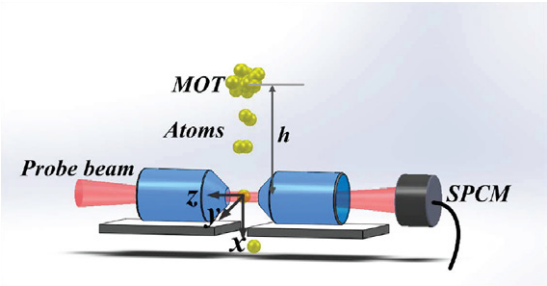

Figure 1. Schematic of our experimental setup. The microcavity consists of two super-mirrors. The cold atom cloud is produced in a MOT right above the centre of the cavity. The SPCM is used to detect the cavity output. Atoms fall freely from the MOT under gravity and pass through the cavity mode.

ultrahigh-vacuum (UHV) cell was maintained at about 1×10^{-10} Torr. The Fabry–Perot cavity here had a high finesse of $F = 3.3 \times 10^5$, and was composed of two super-polished spherical mirrors with a radius of curvature of 100 mm and an end-diameter of 1 mm. The cavity length l was 86.9 μm [14] and the waist of the intra-cavity TEM_{00} mode at 852.356 nm was $\omega_0 = 23.8$ μm. Our system operated in a strong coupling regime with the parameters $g_0 = 2\pi \times 23.9$ MHz, $\kappa = 2\pi \times 2.6$ MHz, $\gamma = 2\pi \times 2.6$ MHz for the TEM_{00} mode, where g_0 is the peak atom–field coupling coefficient between the cavity TEM_{00} mode and atoms, and κ, γ are the cavity and atom decay rates, respectively. A weak probe laser beam of 852 nm was tuned close to the transition of the cesium D_2 line $6^2S_{1/2}$, $F = 4 \rightarrow 6^2P_{3/2}$, $F' = 5$. An auxiliary 828 nm diode laser was applied to lock the length of the microcavity, and self-stabilized relative to the transition of the cesium D_2 line by a 'transfer cavity'. The output of the cavity was of the order of picowatts, and was measured using a single-photon counting module (SPCM) (Perkin Elmer Model SPCM-AQR-15) with a total photon detection efficiency of $\eta = 7.5\%$, which included the efficiencies of the cavity emission, beam propagation and photodetection.

In the experiment, approximately 4×10^4 atoms were initially accumulated by laser cooling in the MOT, which was located about 6 mm right above the center of the microcavity. The atoms were further cooled down using polarization gradient cooling (PGC). They then dropped down freely in the presence of gravity, at the same time strongly interacting with the cavity mode which led to a tremendous change in the cavity transmission. That is, the presence of an atom inside the microcavity brought about a sudden drop in the transmission, as illustrated in figure 2. Typical emission signals of the cavity without and with PGC are shown in figures 2(a) and (b) at temperatures of $T = 197.5 \pm 2.28$ μK and $T = 31.3 \pm 0.7$ μK, respectively. The atomic temperatures were determined by the method we proposed in 2011 [15]. The probe field with an average intracavity photon number of about 1 was resonant with the cavity. Because a dip in the cavity emission (blue squares) in figures 2(a) and (b) corresponded to the arrival of an atom in the cavity, single-atom events could be extracted from the cavity emission recorded by a real-time detector. Figures 2(c) and (d), corresponding to figures 2(a) and (b), respectively, illustrates the arrival times of the atoms more clearly.

To identify the single-atom events more effectively from the transmission spectra, we needed to define a reasonable threshold (illustrated by the gray-dashed line in figure 2), that is to say, only when the photon count was below the defined threshold, were the events caused by atom transits. Therefore we compared the extracted atom transits using two and four times the standard deviation of the photon noise as a threshold. In figure 3, the atom events could be more correctly extracted when the threshold was taken as four times the standard deviation of the photon noise (blue bars) than for twice (black bars). As an example, we can determine the exact atom events, given by the blue squares in figures 2(a) and (b) and then record the exact arrival times, displayed by the red sticks in figures 2(c) and (d). The value of this threshold was calculated to be set at four times the shot noise of the probe laser, shown by the gray-dashed line in figures 2(a) and (b). Thus we were able to record a number of two-dimensional arrays including the atom arrival time and photon counts (the depth of the falling dips). For these atom events, the transmission reduction, compared with the average photon number, was then obtained and the frequency of the same reduction acquired, as illustrated in figure 3 (color bars).

Figure 4(a) shows the second-order correlation function $g^{(2)}(\tau) = \langle I(t)I(t+\tau)\rangle/\langle I(t)\rangle^2 = P_c(t \mid t+\tau.)$ [16] of truly thermal atomic beams at different temperatures, derived from the arrival times of the atoms. For the higher (lower) temperature atom cloud without (with) PGC we obtained the green triangle (blue diamond) curve. The orange and red lines were fitted to the experimental results according to the theory of multimode thermal field coherence. Here we assumed a Gaussian multimode thermal field, so the normalized second-order coherence function is given by [16]:

$$g^{(2)}(\tau) = 1 + |g^{(1)}(\tau)|^2 = 1 + \left|\exp\left(-i\omega_0\tau - \frac{1}{2}\delta^2\tau^2\right)\right|^2$$
$$= 1 + \exp(-\delta^2\tau^2) \quad (1)$$

where δ is the spectral linewidth and ω_0 the central frequency. It was evident that the degree of second-order coherence $g^2(\tau) \geqslant 1$, and $g^2(\tau)\,|_{\max} = 2$ at $\tau = 0$. Here, we used the function $g^{(2)}(\tau) = 1 + \beta\ \exp(-\tau^{\ 2}/\eta^{\ 2})$ to fit the experimental data in figure 4(a), where the linewidth η was dependent on the temperature of the atoms, and the coefficient β was mainly caused by the limited signal-to-noise ratio in photodetection, as well as fluctuations in the magnetic field and probe laser. The η was used to describe the width of the Gaussian spectrum and increased with the number of modes. From our theoretical fit, we obtained $\eta = 23.7 \pm 0.12$ ms, $\beta = 0.55$ for the atomic beam without PGC and $\eta = 14.9 \pm 0.09$ ms, $\beta = 0.55$ with PGC. Figures 4(b) and (c) denote the probability distributions of the number of events N with a time interval of $T = 20.7$

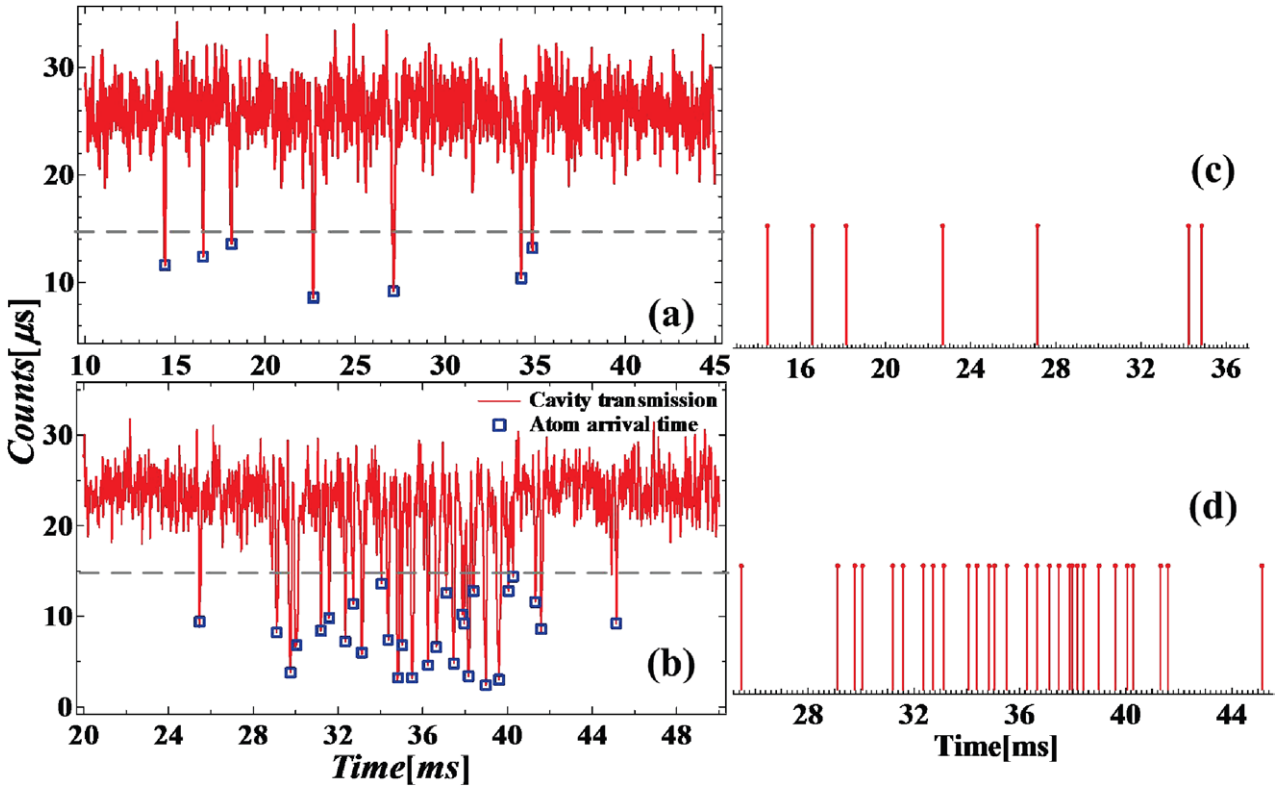

Figure 2. Cavity emission signals from two cold atom samples detected by the SPCM: (a) without PGC and (b) with PGC. The signals from the atoms increased after PGC, and their arrival time was delayed when other conditions were the same. The red curve is the direct output from the SPCM, and a sudden drop in cavity emission (blue squares) corresponded to the arrival of an atom in the cavity. Figures 2(c) and (d), corresponding to figures 2(a) and (b), respectively, illustrate the arrival times of the atoms more clearly.

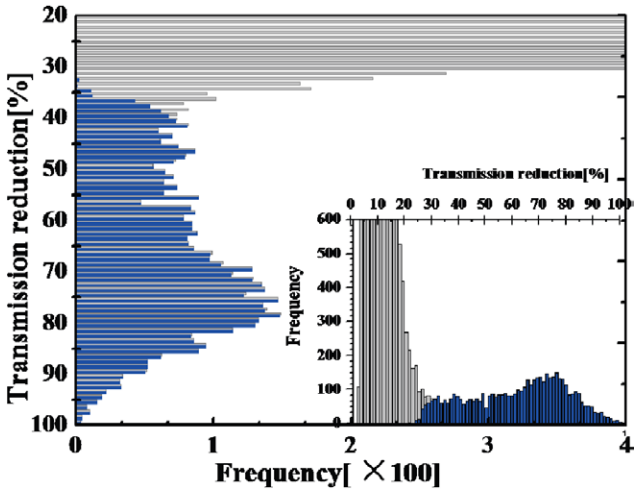

Figure 3. Distribution of measured cavity transmission reduction magnitudes. The black bars indicate the extracted atom signal from setting twice the threshold, and the blue bars are for four times the threshold. The inset illustration shows the enlarged view. It proved that four times the standard deviation of the photon shot noise as the threshold was better for recognizing a real atom event than twice the standard deviation.

ms for the atomic beam after PGC, and $T = 28.5$ ms without PGC. The crosses (+) indicate a Bose distribution of $p(N) = \langle n\rangle^N/(1 + \langle n\rangle)^{1+N}$, which was to be expected for a thermal event with the same mean value of $\langle n\rangle = 1.97$.

In an analogy with thermal light, the spectral width became wider as the atomic temperature increased, which stemmed from the change in the number of atomic modes. Although the two atomic clouds had different initial temperature distributions and consequently different decay rates, both their second-order correlation functions exhibited the bunching effect of a truly thermal atomic beam.

3. Conclusions

The correlation statistics of neutral ^{133}Cs atoms were investigated in a strongly coupled cavity QED system. Here, two atom samples were considered with different initial temperatures, one sample with and the other without undergoing PGC. The atom–atom correlation statistics exhibited a bunching effect similar to thermal optical beams. The second-order correlation function of a multimode thermal optical beam was used to fit the experiment data for the atom beams. As with chaotic thermal light, we found that the atom correlation time was dependent on the atom mode number, controlled by the initial temperature in the MOT [17]. The relevant parameter values were obtained by the theoretical fitting of the experimentally measured curves. The cavity QED system enabled us to observe the statistical distribution and correlation of a true thermal atom beam using single-photon counting techniques.

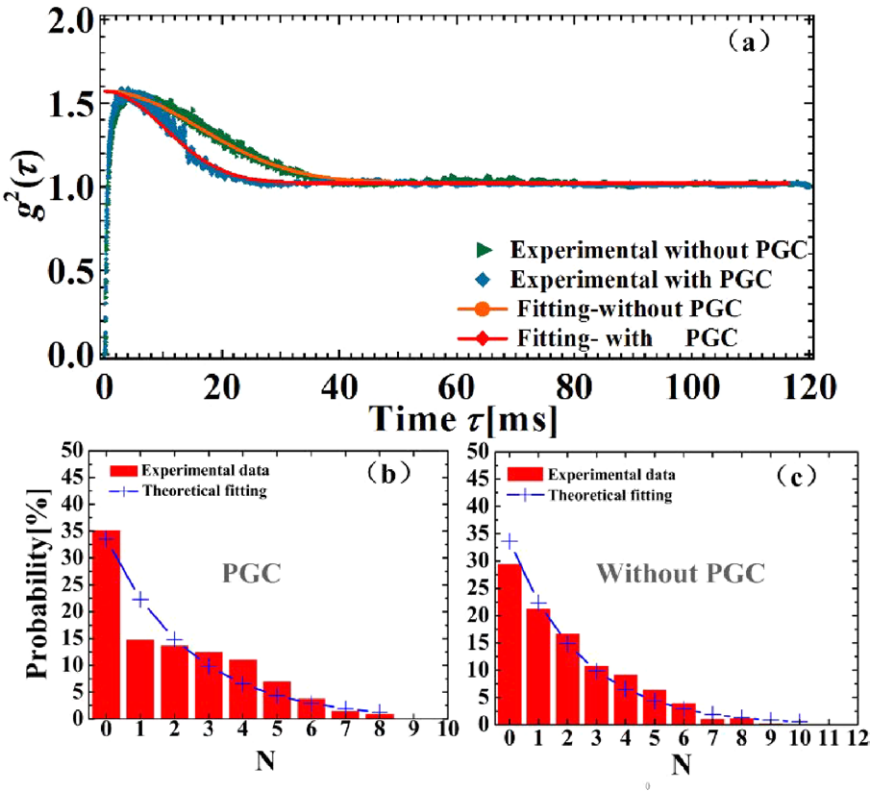

Figure 4. (a) Second-order correlation functions of truly thermal atomic beams. The green triangle line is without PGC, the blue diamond line with PGC. The orange and red lines are the corresponding curves fitted according to the theory of multimode thermal field coherence. (b),(c) The probability distribution of the number of events N for a time interval of $T = 20.7$ ms after PGC (b), and $T = 28.5$ ms without PGC (c). The crosses (+) indicate a Bose distribution with the same mean value of $\langle n \rangle = 1.97$.

Acknowledgments

We thank Professor L-A Wu for her reading the article and giving some suggestions. This work is supported by the National Basic Research Program of China (Grant No. 2012CB921601), and the NSFC (Grant Nos. 11125418, 61227902, 61275210, 91336107, 61121064).

References

[1] Hanbury Brown R and Twiss R Q 1956 *Nature* **178** 1046
[2] Phelan D *et al* 2007 *Astrophysics and Space Science Library* (Berlin: Springer)
[3] Glauber R J 1965 *Quantum Optics and Electronics* (New York: Gordon and Breach)
[4] Yasuda M and Shimizu F 1996 *Phys. Rev. Lett.* **77** 3090
[5] Schellekens M *et al* 2005 *Science* **310** 648
[6] Ottl A *et al* 2005 *Phys. Rev. Lett.* **95** 090404
[7] Manning A G *et al* 2010 *Opt. Express* **18** 018712
[8] Dall R G *et al* 2011 *Nat. Commun.* **2** 291
[9] Jeltes T *et al* 2007 *Nature* **445** 402
[10] Hood C J *et al* 1998 *Phys. Rev. Lett.* **80** 4157
[11] Munstermann P *et al* 1999 *Opt. Commun.* **159** 63
[12] Du J J *et al* 2013 *Appl. Phys. Lett.* **103** 083117
[13] Li W F *et al* 2014 *Appl. Phys. Lett.* **104** 113102
[14] Du J J *et al* 2013 *Acta Phys. Sin.* **62** 194203
[15] Zhang P F *et al* 2011 *J. Opt. Soc. Am.* B **28** 667
[16] Walls D F and Milburn F J 1995 *Quantum Optics* (Berlin: Springer)
[17] Wang J L *et al* 2015 *J. Quantum Opt.* **21** 74